

# Protein chemical shifts arising from $\alpha$ -helices and $\beta$ -sheets depend on solvent exposure

Franç Avbelj<sup>\*†</sup>, Darko Kocjan<sup>‡</sup>, and Robert L. Baldwin<sup>†§</sup>

<sup>\*</sup>National Institute of Chemistry, Hajdrihova 19, SI 1115 Ljubljana, Slovenia; <sup>†</sup>Lek Pharmaceutical Company, d.d., Verovskova 57, SI 1000 Ljubljana, Slovenia; and <sup>§</sup>Biochemistry Department, Beckman Center, Stanford University Medical Center, Stanford, CA 94305-5307

Contributed by Robert L. Baldwin, October 26, 2004

The NMR chemical shifts of certain atomic nuclei in proteins ( $^1\text{H}_\alpha$ ,  $^{13}\text{C}_\alpha$ , and  $^{13}\text{C}_\beta$ ) depend sensitively on whether or not the amino acid residue is part of a secondary structure ( $\alpha$ -helix,  $\beta$ -sheet), and if so, whether it is helix or sheet. The physical origin of the different chemical shifts of atomic nuclei in  $\alpha$ -helices versus  $\beta$ -sheets is a problem of long standing. We report that the chemical shift contributions arising from secondary structure (secondary structure shifts) depend strongly on the extent of exposure to solvent. This behavior is observed for  $^1\text{H}_\alpha$ ,  $^{13}\text{C}_\alpha$ , and  $^{13}\text{C}_\beta$  (sheet), but not for  $^{13}\text{C}_\beta$  (helix), whose secondary structure shifts are small. When random coil values are subtracted from the chemical shifts of all  $^1\text{H}_\alpha$  nuclei (Pro residues excluded) and the residual chemical shifts are summed to plot the mean values against solvent exposure, the results give a funnel-shaped curve that approaches a small value at full-solvent exposure. When chemical shifts are plotted instead against  $E_{\text{local}}$ , the electrostatic contribution to conformational energy produced by local dipole–dipole interactions, a well characterized dependence of  $^1\text{H}_\alpha$  chemical shifts on  $E_{\text{local}}$  is found. The slope of this plot varies with both the type of amino acid and the extent of solvent exposure. These results indicate that secondary structure shifts are produced chiefly by the electric field of the protein, which is screened by water dipoles at residues in contact with solvent.

protein solvation | secondary structure shifts

The chemical shift index method (1, 2) is commonly used to assign protein secondary structures. This method is based on the secondary structure shift, which is the difference between the observed chemical shift and the random coil value assigned to this amino acid type in the unfolded conformation. Assignment of secondary structure is a useful intermediate step in determining the 3D solution structure of a protein from NMR data. Secondary structure assignment is also useful in predicting the 3D structure of a protein from its amino acid sequence. A threading method based on chemical shift data has been developed (2) for testing whether an amino acid sequence can fold to form a given 3D structure. Understanding the origin of the distinctive secondary structure shifts of helices and sheets is a problem of considerable interest.

Protein chemical shifts, for a given atomic nucleus and amino acid type, display large variations, and the factors that control these variations are poorly understood. The reason why the chemical shift index method works so well for assigning secondary structures is that the secondary structure shift has opposite signs for  $\alpha$ -helix and  $\beta$ -sheet (1–3). Several proposals have been made (4–10) regarding the physical origin of the different chemical shifts found in  $\alpha$ -helices and  $\beta$ -sheets. For both the  $^1\text{H}_\alpha$  and the  $^{13}\text{C}_\alpha$  nuclei, protein chemical shifts are said to depend chiefly on  $\phi, \psi$  torsion angles and on the random coil values (2). The protein electric field may contribute to chemical shifts (5), but its contribution is difficult to evaluate and screening of the electric field by solvent has not yet been taken into account (5). Current estimates of the factors influencing secondary structure shifts (2) treat solvent exposure as a minor factor. There are now sufficient chemical shift entries in the BioMagResBank database

(11) to examine this issue directly by computing solvent exposure for these entries and analyzing the results.

## Dependence of Chemical Shifts on Exposure to Solvent

Fig. 1A displays the dependence of  $^1\text{H}_\alpha$  chemical shift on solvent exposure for different amino acid types. Data for 1,010 proteins, obtained from the BioMagResBank database (11) are shown. Secondary structure is assigned by the DSSP algorithm (12) and the random coil shifts are from ref. 2. Similar results are found for  $^{13}\text{C}_\alpha$  (Fig. 1B) and  $^{13}\text{C}_\beta$  (sheet) (Fig. 1C). Two levels of solvent exposure are shown: buried (solvent exposure of  $<0.1$ ) and partially exposed (solvent exposure of  $>0.4$ ). Because the chemical shifts are obtained from studies of native protein structures, very few chemical shifts are reported for fully exposed residues. The exposure to solvent is computed from the solvent-accessible surface area (ASA) (13), with full solvent accessibility being defined from the ASA values of a stochastic mixture of tripeptides (14). Although the stochastic mixture of tripeptides is fully solvent-exposed by the definition (14) used here, even peptide groups in tripeptides experience partial shielding from water by neighboring side chains and residue X has a solvent exposure of  $>1$  in a peptide with glycine on either side of X, GXG.

Fig. 1 shows that substantial solvent exposure causes the absolute values of secondary structure shifts to decrease significantly. Similar results are found for  $\alpha$ -helix and  $\beta$ -sheet, for  $^1\text{H}_\alpha$  (Fig. 1A),  $^{13}\text{C}_\alpha$  (Fig. 1B), and  $^{13}\text{C}_\beta$  (sheet) (Fig. 1C), and for all 18 aa considered. Gly and Pro are omitted because they have very small propensities for forming  $\alpha$ -helices and  $\beta$ -sheets. Only small secondary structure shifts are found for  $^{13}\text{C}_\beta$  (helix) (Fig. 1C), and there is no clear dependence on solvent exposure. The reason why the  $^{13}\text{C}_\beta$  chemical shift differences are small for helical residues is not known, but a relevant factor is that  $\text{C}_\beta$  is further from the helix backbone than  $^{13}\text{C}_\alpha$  and  $^1\text{H}_\alpha$ .

To plot mean values of residual chemical shift versus solvent exposure, data for 19 aa (Pro excluded) were summed and all residues, both within and outside secondary structure, are included in Fig. 2. The chemical shift difference refers to the observed value minus the random coil value. Subtraction of random coil values yielded roughly equal numbers of residues with positive and negative chemical shift differences. The positive and negative values were processed separately. Chemical shift results (11) for 103,084  $^1\text{H}_\alpha$  nuclei were analyzed. The data were binned by using a bin size of 0.1 in solvent exposure. The mean (absolute) values of chemical shift difference decreased regularly with increasing solvent exposure. They approached small values for solvent exposure of  $>1.4$ , where the funnel-shaped plot ends because there were  $<20$  residues per bin. As explained above, the standard definition of solvent exposure (14) allows values of  $>1.0$  to be observed for some sequences. The rms deviation values are plotted in Fig. 2, and they also show a

Abbreviations: ASA, solvent-accessible surface area; ESF, electrostatic solvation free energy.

<sup>†</sup>To whom correspondence may be addressed. E-mail: franc@sg3.ki.si or rbaldwin@cmgm.stanford.edu.

© 2004 by The National Academy of Sciences of the USA



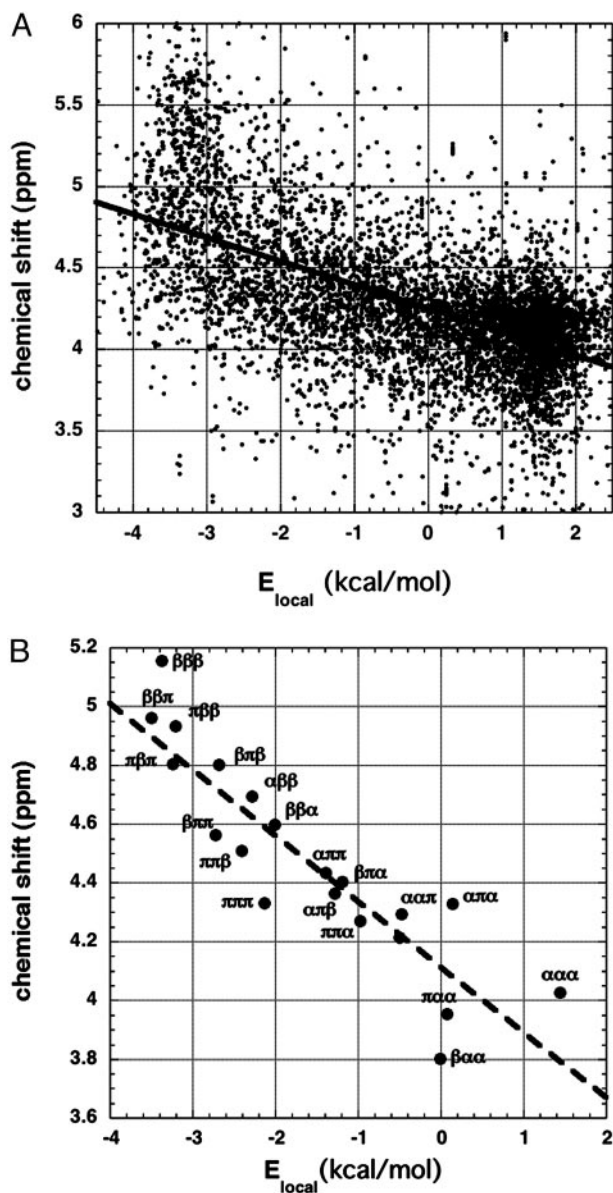


**Fig. 3.** The plot of individual chemical shift values against  $E_{\text{local}}$  for all alanine residues (A) and for the central residues of selected triplet sets composed of three main core backbone conformations (B). (A)  $^1\text{H}_\alpha$  chemical shift versus  $E_{\text{local}}$  (ref. 15; see text) for 7,548 alanine residues in protein structures. Data are from the BioMagResBank database (11). (B) Mean values of chemical shift and  $E_{\text{local}}$  are shown for each alanine triplet type by using only residues in core regions of the three main backbone conformations,  $\alpha$ ,  $\beta$ , and  $\pi$  (polyproline II). The rms deviation values, which are large, vary from 0.24 ppm for  $\alpha\alpha\alpha$  to 0.53 ppm for  $\beta\pi\beta$ . The definitions (27) of core  $\alpha$ ,  $\beta$ , and  $\pi$  are based on  $\phi, \psi$  values taken from the Ramachandran maps of the amino acid types (27);  $\beta$  is to the left and  $\pi$  is to the right of  $\phi = -100^\circ$ . There are 273 alanine residues in the  $\beta\beta\beta$  triplet and 2,776 residues in the  $\alpha\alpha\alpha$  triplet. The line is taken from A.

is a large range of values of chemical shift at each value of  $E_{\text{local}}$  and the correlation between chemical shift and  $E_{\text{local}}$  accounts for only part of this range, we made the following test of the correlation between  $E_{\text{local}}$  and chemical shift. Sets of three consecutive residues (triplets) were analyzed that contain mixed sequences of the three main backbone core conformations ( $\alpha$ ,  $\beta$ , and  $\pi$ ) found in protein structures. The core conformations are defined by  $\phi, \psi$  values and are based on observed occupancies of regions of the Ramachandran map (see the Fig. 3B legend for definitions). The average chemical shift of the central residue in each triplet type ( $\beta\alpha\beta$ ,  $\pi\beta\alpha$ , etc.) is

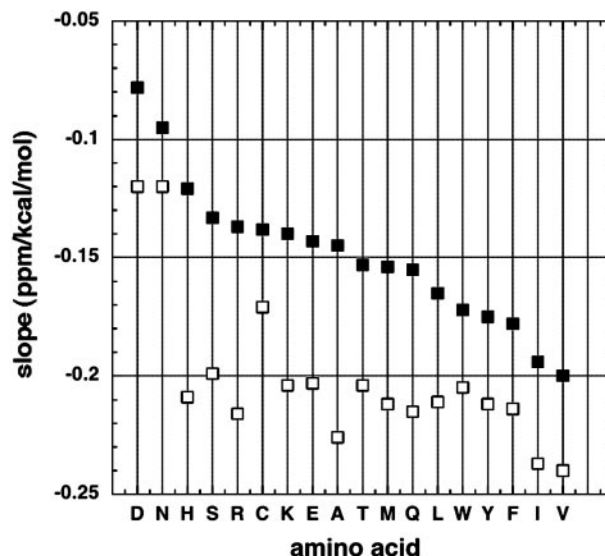


**Fig. 4.** Plots like Fig. 3A are made for the different amino acid types and the slope of each plot is displayed against amino acid type for two classes of plot: (i) all residues are used (■) and (ii) only buried residues (solvent exposure of  $<0.1$ ) are used (□).

plotted against the average value of  $E_{\text{local}}$  for that triplet type in Fig. 3B. The specific triplet results cluster around the line determined for all residue types (from Fig. 3A), which indicates that the dependence of average chemical shift on  $E_{\text{local}}$  is well characterized.

Because the secondary structure shifts depend strongly on ASA (Figs. 1 and 2), we investigated whether the slopes of the plots of chemical shift versus  $E_{\text{local}}$  (Fig. 3A) also depend on ASA. Fig. 4 compares values of the slope ( $S$ ) for different amino acid types, both for buried residues (solvent exposure of  $<0.1$ ) and for partially exposed residues (solvent exposure of  $>0.4$ ). The results in Fig. 4 show that  $S$  depends strongly on both amino acid type and extent of solvent exposure. Negative values of  $S$  are larger for buried residues than for partially exposed residues, and the variation of  $S$  with amino acid type is stronger for partially exposed than for buried residues. For at least 13 aa types (H–F, omitting C, in Fig. 4), the buried-residue values of  $S$  are nearly constant.

#### Nature of the Relation Between Chemical Shift and Solvent Exposure

Two explanations may be invoked for the relation between chemical shift and solvent exposure. The secondary structure shifts may be produced by the protein electric field, which is screened by water dipoles at residues in contact with solvent. Or the secondary structure shifts might be caused by close non-bonded contacts, for which increased solvent exposure would cause the magnetic shielding to decrease. However, an increase in solvent exposure causes an increase in  $^1\text{H}_\alpha$  shielding for  $\beta$ -sheet residues (Figs. 1A and 2). Consequently, the protein electric field is the probable main cause of the secondary structure shifts, for example, the electric field may polarize the peptide C=O bond in chains of H bonds found in helices and sheets, as suggested recently (9). Note, however, that in this study (9) contact with solvent and the polarizing action of water dipoles is not taken into account.

If the electric field is the cause of secondary structure shifts, then the various values of  $S$  for different amino acid types in Fig. 4 should reflect the differing abilities of these amino acids to shield neighboring peptide groups from solvent, because screening of the electric field by water dipoles at a given site depends on the extent to which the peptide group at that site is in contact with solvent. When the peptide geometry (including side-chain

rotamers) is defined, the extent to which a given peptide group is shielded from interacting with water is given by its electrostatic solvation free energy (ESF) value (16–19). The ESF value of an amino acid residue is expressed as a negative free energy that gives the strength of interaction between water and the peptide group of this residue. Partial charges on polar side chains are omitted to focus on the polar peptide C=O and NH groups. An ESF value of 0 indicates that the peptide group is completely buried (19), out of contact with water. However, when the first solvation shells of the peptide NH and C=O groups are empty so that ASA = 0, and contact with water is limited to the second and more distant solvation shells, a peptide may nevertheless have a small but finite ESF value (F.A., unpublished data).

The electrostatic algorithm DELPHI (20) has been used to compute the ESF values of various peptide conformations (16–19), and the results have been compared (17) with results found with an algorithm based on a Langevin dipole treatment (21). The parameters of DELPHI (partial charges and atomic radii) are left invariant in these calculations and the ESF value of a residue is determined by the peptide geometry of the peptide and the access of water to the peptide group.

To test the proposal that differences in the slope  $S$  among amino acids (Fig. 4) depend on the water-shielding properties of the amino acid side chain, values of  $S$  for partially exposed residues are plotted in Fig. 5 against the thermodynamic  $\beta$ -propensity of the amino acid. A fairly good correlation (correlation coefficient of 0.72) is found. The reason for testing whether a correlation is found is that  $\beta$ -propensities are well correlated with ESF values (19) in a study of mutants of a zinc finger protein. This system has been used to provide values for thermodynamic  $\beta$ -propensities (22). Amino acids with strongly shielding side chains, according to ESF values, include the  $\beta$ -branched and aromatic amino acids (FHITVWY) (16, 19), which have high  $\beta$ -propensities (22). The experimental ESF values of amides are not related in any simple way to their polar ASA values (18), however, and there is only a moderate correlation between ESF and solvent exposure for the residues whose  $^1\text{H}_\alpha$  chemical shifts (Fig. 2) are studied here (data not shown).

### Relation of These Results to Predictions and Uses of Protein Chemical Shifts

Random coil values of chemical shifts are used to help in assigning resonances in spectra of denatured proteins and to test for the presence of residual structure (23, 24). The name “random coil” implies that no single backbone conformation is preferred and the argument has been made (25) that the  $\beta$ -strand conformation is not found as a regular, repeating conformation in unfolded peptides, although it is favored by peptide dipole–dipole interactions (15), because it would be detected by the  $^1\text{H}_\alpha$  secondary shift characteristic of  $\beta$ -structure. Our results demonstrate that  $^1\text{H}_\alpha$  secondary

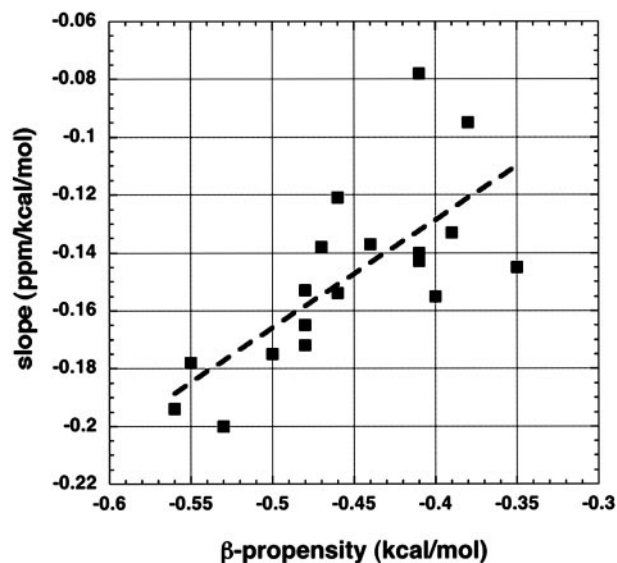


Fig. 5. The slope found in all-residue plots (see Figs. 3A and 4) is displayed against the thermodynamic  $\beta$ -propensity (22) of the amino acid type. The thermodynamic  $\beta$ -propensities were measured (22) from the unfolding free energies of mutants for a site within a partially solvent-exposed  $\beta$ -hairpin of a zinc finger protein. The thermodynamic  $\beta$ -propensities correlate well (22) with statistical frequencies in  $\beta$ -sheets. The slopes shown are displayed against amino acid type in Fig. 4.

structure shifts become small for solvent-exposed residues such as those present in short peptides. Thus, solvent exposure must be a major factor determining the values of random coil shifts found in short peptides, and secondary structure shifts might pass undetected because they are small. The surprisingly wide range of values found for secondary structure shifts in proteins has been a puzzle in using the chemical shift index method (1, 2). Our results pinpoint two factors (solvent exposure and  $E_{\text{local}}$ ) that contribute to this wide range.

The Buckingham equation (26) predicts that the local electric field is the key variable determining the electrostatic contribution to  $^1\text{H}_\alpha$  secondary structure shifts. Our results make it clear that solvent screening of the electric field must be included to predict chemical shifts for proteins. Research needs to be performed to test possible computational models for obtaining the local electric field, which is obtained by numerical differentiation of the electrostatic potential.

We thank S. Boxer, S. Golic Grdadolnik, D. Hadzi, J. Hermans, I. Kuntz, P. Pristovsek, and D. Wemmer for discussion. This work was supported by a grant from the Ministry of Education, Science and Sport of Slovenia and Lek Pharmaceutical Company, d.d.

- Wishart, D. S., Sykes, B. D. & Richards, F. M. (1992) *Biochemistry* **31**, 1647–1651.
- Wishart, D. S. & Case, D. A. (2001) *Methods Enzymol.* **338**, 3–34.
- Spera, S. & Bax, A. (1991) *J. Am. Chem. Soc.* **113**, 5490–5492.
- Ösapay, K. & Case, D. A. (1991) *J. Am. Chem. Soc.* **113**, 9436–9444.
- Dios, A. C. D., Pearson, J. G. & Oldfield, E. (1993) *Science* **260**, 1491–1496.
- Williamson, M. P. & Asakura, T. (1993) *J. Magn. Reson.* **101**, 63–71.
- Ösapay, K. & Case, D. A. (1994) *J. Biomol. NMR* **4**, 215–230.
- Asakura, T., Taoka, K., Demura, M. & Williamson, M. P. (1995) *J. Biomol. NMR* **6**, 227–236.
- Thomas, A., Milon, A. & Brasseur, R. (2004) *Proteins* **56**, 102–109.
- Sitkoff, D. & Case, D. A. (1997) *J. Am. Chem. Soc.* **119**, 12262–12273.
- Seavey, B. R., Farr, E. A., Westler, W. M. & Markley, J. L. (1991) *J. Biomol. NMR* **1**, 217–236.
- Kabsch, W. & Sander, C. (1983) *Biopolymers* **22**, 2577–2637.
- Lee, B.-K. & Richards, F. M. (1971) *J. Mol. Biol.* **55**, 379–400.
- Shrake, A. & Rupley, J. A. (1973) *J. Mol. Biol.* **79**, 351–371.

- Avbelj, F. & Moult, J. (1995) *Biochemistry* **34**, 755–764.
- Avbelj, F. & Baldwin, R. L. (2004) *Proc. Natl. Acad. Sci. USA* **101**, 10967–10973.
- Avbelj, F. (2000) *J. Mol. Biol.* **300**, 1335–1359.
- Avbelj, F., Luo, P. & Baldwin, R. L. (2000) *Proc. Natl. Acad. Sci. USA* **97**, 10786–10791.
- Avbelj, F. & Baldwin, R. L. (2002) *Proc. Natl. Acad. Sci. USA* **99**, 1309–1313.
- Sitkoff, D., Sharp, K. A. & Honig, B. (1994) *J. Phys. Chem.* **98**, 1978–1988.
- Florian, J. & Warshel, A. (1997) *J. Phys. Chem. B* **101**, 5583–5595.
- Kim, C. A. & Berg, J. M. (1993) *Nature* **362**, 267–270.
- Dyson, H. J. & Wright, P. E. (2002) *Adv. Protein Chem.* **62**, 311–340.
- Schwarzinger, S., Kroon, G. J. A., Foss, T. R., Chung, J., Wright, P. E. & Dyson, H. J. (2001) *J. Am. Chem. Soc.* **123**, 2970–2978.
- Bai, Y., Chung, J., Dyson, H. J. & Wright, P. E. (2001) *Protein Sci.* **10**, 1056–1066.
- Buckingham, A. D. (1960) *Can. J. Chem.* **38**, 300–307.
- Morris, A. L., MacArthur, M. W., Hutchinson, E. G. & Thornton, J. M. (1992) *Proteins* **12**, 345–364.